ARCHIVES OF ACOUSTICS
13, 1–2, 13–43 (1988)

TUTORIAL

SCANNING ACOUSTIC MICROSCOPY OF POLYMERIC MATERIALS AND BIOLOGICAL SUBSTANCES

ROMAN GR. MAYEV

Center of Acoustic Microscopy, USSR Academy of Sciences Institute of Chemical Physics, USSR, Moscow, 117334 Kosygin str. 4

For the last few years a new method of visualization and quantitative analysis of physico-mechanical properties and microstructure of heterogenetic media – the acoustic microscopy – has been intensively elaborated in the world. In this method waves of ultrasound and hypersound range are used as an analysis factor. It allows to use this method for investigating a wide variety of opaque materials and goods and obtaining information about their inner structures as well as for optically transparent materials in which the contrast between different structures is practically absent. In both cases an investigator receives information that is quite different from that obtained with the help of other methods, namely, the distribution of local physico-mechanical properties for example, bulk compression, shift, etc in the material of the sample.

We give a review of the results of the work on methods and means of acoustic microscopy, worked out in the Centre for Acoustic Microscopy of the USSR Academy of Sciences for investigation of polymeric composites and biological objects as well as the results of analogical investigations of the loading scientific centres in the world.

We set forth common physical basis and principles of getting acoustic images as well as the methods of studying microstructures and mechanical properties of heterogenetic objects with the help of acoustic microscope.

W ciągu ostatnich lat rozwijana jest na świecie akustyczna mikroskopia – nowa metoda wizualizacji i analizy jakościowej własności fizykomechanicznych i mikrostruktury ośrodków niejednorodnych. W metodzie tej stosowane są fale o częstotliwościach ultra- i hiperdźwiękowych. Pozwala to na badanie zarówno różnych nieprzezroczystych materiałów i przedmiotów i uzyskanie informacji o ich wewnętrznych strukturach, jak również badanie materiałów optycznie przezroczystych, w których nie ma praktycznie kontrastu pomiędzy różnymi strukturami. W obu przypadkach badacz uzyskuje informacje całkowicie różne od otrzymanych za pomocą innych metod, a mianowicie rozkład lokalnych własności fizykomechanicznych np. ściśliwość objętościowa, przesunięcie w materiale próbki.

W artykule podajemy przegląd wyników prac wykonanych w Centrum Mikroskopii Akustycznej Akademii Nauk ZSRR i obejmujących akustyczną mikroskopię kompozytów

polimerowych i obiektów biologicznych oraz wyniki analogicznych badań uzyskanych przez przodujące ośrodki naukowe na świecie.

Opracowaliśmy zarówno podstawy fizyczne i zasady uzyskiwania obrazów akustycznych, jak również metody badania mikrostruktur i własności mechanicznych ośrodków niejednorodnych za pomocą mikroskopii akustycznej.

1. Introduction

Today there are several sufficiently effective methods for investigating physico-chemical morphology and the local distribution of microstructures in polymeric mixtures and biological substances. The most important among them are optical and electron microscopic methods.

The present work is an analysis of the possibilities of a fundamentally new method, scanning acoustic microscopy SAM, for studying the physico-mechanical microstructure and dynamic processes in materials of the most diverse nature.

2. Principles of Scanning Acoustic Microscopy (SAM)

Let us first recall the principles of acoustic microscopy (Fig. 1). A high radio frequency pulse from a piezoelectric transducer is focused by an acoustic lens in a liquid coupling medium. The lens is in the form of a spherical cavity at the end of the soundguide. On interacting with the sample a focused beam is partially reflected from the sample and partially passes through it. In the former case we have a reflecting microscope; and in the latter case, after the beam passes through a second lens, we have a transmission acoustic microscope. Subsequent operations include the scanning of the sample relative to the focal region, recording the signal at every point and storing the signal in memory unit, synchronizing the sweep with the scanning, and using the signal to control the intensity of the electron beam. These operations result in the formation of an acoustic image on the display screen.

The interaction of sound wave and the sample yields information that is quite different from that obtained with the help of optical and electron microscopy. This is due to the fundamental difference in the physical nature of ultrasound which manifests itself in the form of elastic deformation waves in a medium. The mechanical nature of ultrasound makes it possible to obtain new information on the mechanical properties of an object with the help of SAM, as distinct from other methods.

The most important characteristics of the SAM method are its resolving power and depth of penetration into the sample. They depend on the frequency of ultrasound, the performance of the lens system, the nature of immersion medium and the properties of the material under investigation etc. With an increase in resolution, the depth of penetration of ultrasound into the sample decreases. Therefore, the frequency of ultrasound should be selected according to the given type of sample and

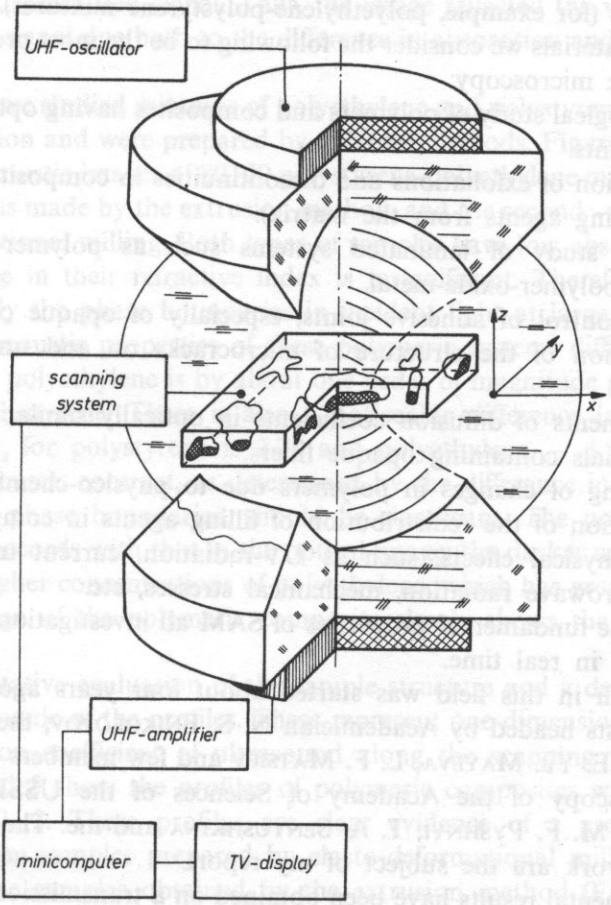

FIG. 1. Principal scheme of transmission scanning acoustic microscope (SAM)

the purpose of the investigation, with a compromise being made between the resolving power and the degree of penetration.

The method of scanning acoustic microscopy is highly sensitive to the presence of various heterogeneities to the appearance of discontinuities, exfoliation and phase boundaries. Owing to mismatch in acoustic impedance there appear strong reflections from the interfaces.

3. SAM of Polymer Composite Materials

Acoustic microscopy has been used in studying the morphology of opaque polymers and composites, in evaluating the elastic properties of deformed polymers, as well as in the investigation of polymeric mixtures whose components have similar

optical properties (for example, polyethylene-polystyrene mixtures). For polymeric and composite materials we consider the following to be the most promising areas of applying acoustic microscopy:

1. Morphological study of polymers and composites having optically similar or opaque components.
2. Investigation of exfoliations and discontinuities in composites (for example, exfoliation of filling agents from the matrix).
3. Adhesion study of laminated systems such as polymer-polymer, polymer-metal, and polymer-oxide-metal.
4. Quality control of adhesive joints, especially of opaque composites.
5. Investigation of the structure of microcracks on and under the sample surface.
6. Measurements of diffusion coefficients in optically similar polymers or in composite materials containing opaque fillers.
7. Monitoring of changes in polymers due to physico-chemical effects.
8. Investigation of the redistribution of filling agents in composites resulting from different physical effects, such as UV-radiation, current transmission and exposure to microwave radiation, mechanical stresses, etc.

Owing to the fundamental properties of SAM all investigations can be carried out directly and in real time.

Our research in this field was started about four years ago by a group of polymer specialists headed by Academician N. S. ENIKOLOPOV; the group included D. D. NOVIKOV, E. Yu. MAYEVA, L. F. MATSIEV and few members of our Center of Acoustic Microscopy of the Academy of Sciences of the USSR: V. M. LEVIN O. V. KOLOSOV, M. F. PYSHNYI, T. A. SENYUSHKINA and me. The most important results of this work are the subject of my report.

The experimental results have been obtained on a transmission raster scanning microscope of our own design [1]. The microscope operated at 0.450 GHz, having a resolution of 3μm. An ultra-high-frequency generator was used for the excitation of ultrasound with the aid of a film transducer.

After the ultrasound is focused on the sample it was received by a confocal lens system. This system consisted of two soundguides made of monocrystalline sapphire oriented along z-axis and acoustic lenses at both ends in the form of spherical cavities with a 300 μm radius of the curvature and a 0.8° aperture. The signal from the receiving transducer was fed, following its amplification, through a computer into a memory unit. The sample was secured in the holder of the scanning system. During a period of $\tau = 8$ s the scanning system made it possible to obtain an acoustic image of the sample cross section with a scanning area of from 0.7×0.7 mm to 2×5 mm. In order to get three-dimensional structure one could also change the position of a selected cross section with respect to the sample thickness within the limits of ± 0.5 mm. Following preliminary numerical treatment of the results on a computer the outgoing data was displayed on a TV-screen as a half-tone image and in the form of profiles and histograms. To obtain the image we used only the differences in the

amplitude of the transmitted signal. Thus, the image reflected the variations in the weakening of the signal due both to the difference in absorption and to reflection or scattering.

In our work we studied mixtures of polyethylene and polystyrene which differed in their composition and were prepared by different methods. Figures 2 and 3 show the optical and acoustic images of 80:20 polystyrene-polyethylene mixtures. The first set of mixtures was made by the extrusion method, and the second – by the method of elasto-deformational milling. Both types of samples have low absorption of light, and the difference in their refractive index is insignificant. Therefore, the optical images reveal only the phase boundaries in incident light at large angles. On the other hand, the acoustic properties of these polymeric systems differ considerably: the absorption in polyethylene is by about one order of magnitude greater than the absorption in polystyrene. There is also a noticeable difference in their acoustic impedance: the v_s for polystyrene is 2.28 and polyethylene – 1.91, respectively. Therefore, the acoustic contrast, as determined by the difference in the absorption and reflection at phase boundaries, should be significant. The position of phase boundaries fully accords with that in the optical image: the darker areas correspond to the zones of higher concentrations of polyethylene, which has greater absorption. The acoustic image of the polymeric composite clearly shows the distribution of phases.

For a quantitative evaluation of the sample structure and a description of the inclusions, use is made of the profiles. These represent one-dimensional distribution of the transmission coefficient of ultrasound along the scanning path.

Figures 4 and 5 show the profiles of polymeric composites which have been shown in Figs. 2, 3. These profiles are clear evidence of a greater degree of homogeneity of the samples prepared by elasto-deformational milling (Fig. 5), as compared with the samples obtained by the extrusion method (Fig. 4). On such a profile that is above the line corresponding to the polyethylene absorption, there are peaks which correspond to polystyrene inclusions.

For two-component compositional materials one can by way of illustration offer a simple morphologic description of one inclusion in another. When scanning a sample which is the matrix of substance A with inclusion of substance B, the amplitude of the transmitted ultrasonic wave reflects the variations of attenuation in the focal region of SAM. These variations are determined by the dimensions and physicomechnical properties of heterogeneity. Thus, for inclusion B located in the focal region and having dimensions l_B along the acoustic axis, the amplitude of the signal from the receiving transducer can be described by the following equation:

$$A = A_0 \left(\frac{\varrho_A \varrho_B C_A C_B}{\varrho_A C_A + \varrho_B C_B} \right)^2 \exp(\alpha_A - \alpha_B) l_B,$$

where

α_A absorption coefficient of ultrasound in A medium,

α_B absorption coefficient of ultrasound in B medium,

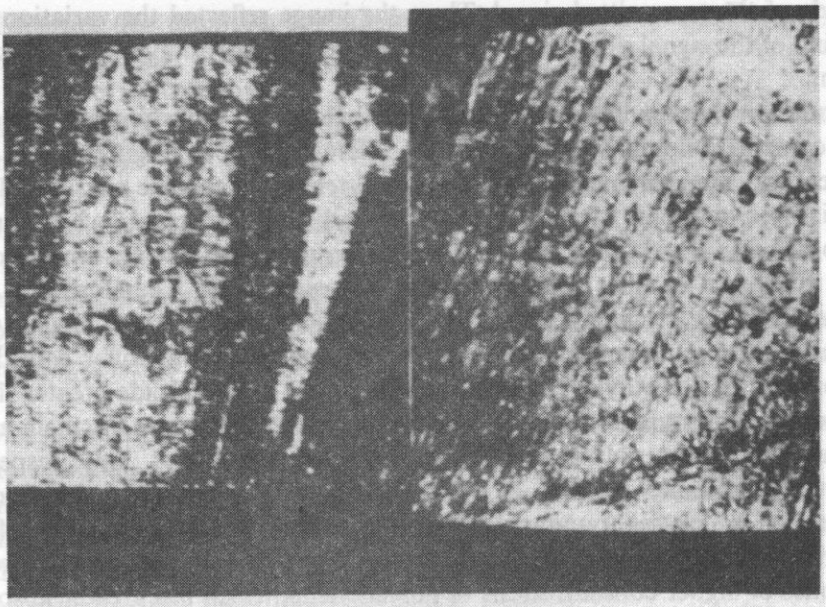

a)

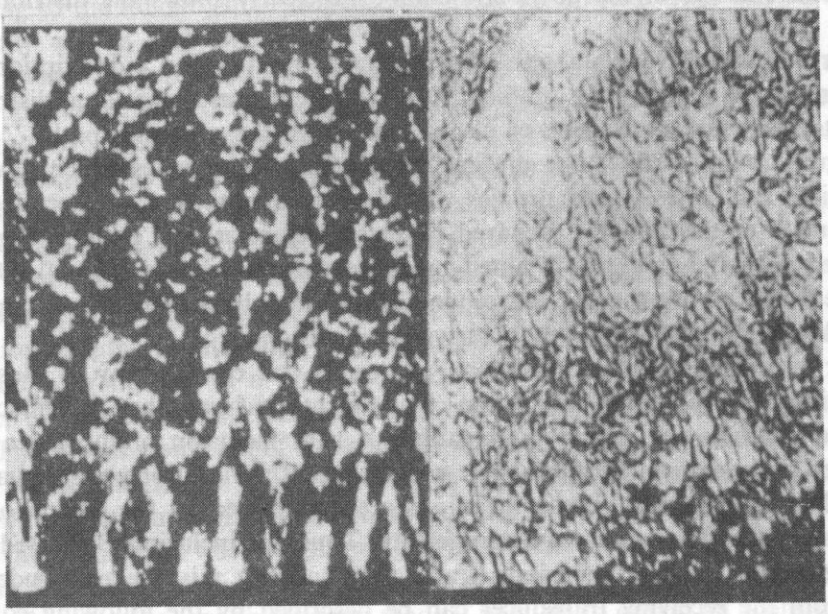

b)

FIG. 2, 3. Acoustic and optical images of 50:50 polystyrene-polyethylene mixtures (a) — mixtures were made by the extrusion method, (b) — by the method of elasto-deformational milling

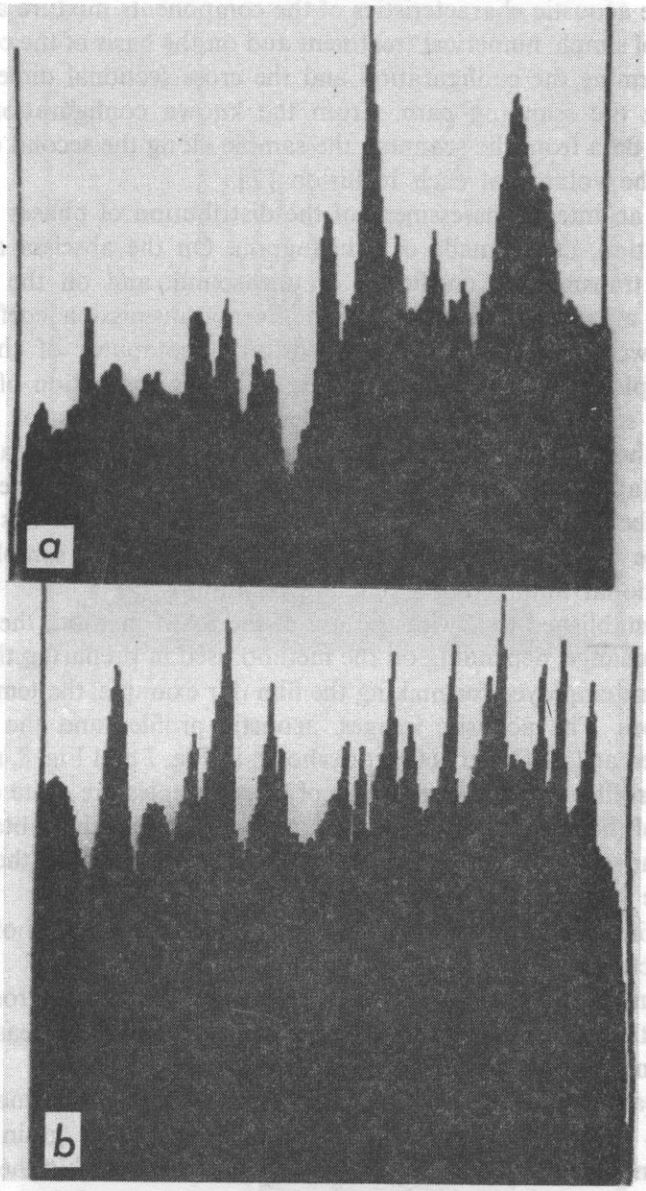

FIG. 4, 5. Profiles of polymeric composites (a) and (b)

ϱ_A density of A medium,
ϱ_B density of B medium,
C_A velocity of ultrasound in A medium,
C_B velocity of ultrasound in B medium,
A_0 amplitude of the signal from the receiving transducer in the absence of inclusion,
A amplitude of the signal when inclusion is present in the focal region.

Thus, if the acoustic characteristics of the components mixture are known, one can, by means of simple numerical treatment and on the basis of the configuration of the peaks, determine the configuration and the cross sectional dimensions of each inclusion along the scanning path. From the known configuration of the cross section and the data from the scanning the sample along the second coordinate one can calculate the volume of each inclusion [2].

To obtain an integral assessment of the distribution of phases in the samples under investigation, use is made of a histogram. On the abscissa are plotted the values for the transmission coefficient of ultrasound, and on the ordinate – a fraction of the area of the sample with a given transmission coefficient.

Fig. 6 shows the histograms obtained on a computer of the two above-mentioned samples of polymeric composite. Since the absorption of ultrasound in polystyrene is smaller than in polyethylene, the properties of inclusions are determined by the wing on the histograms to the right of the main peak. The wing on the histograms (a) is much shorter, and the histogram itself is narrower than (b). This indicates that the heterogeneity of the dimensions of the inclusions in the sample obtained by the extrusion method (b) is greater than in the sample prepared by elasto-deformational milling under cooling conditions (a).

We have established that with the use of the SAM method, the dimensions of heterogeneities change, depending on the method used in preparing the samples and on the conditions employed for making the film (for example, the temperatures used during extrusion). The acoustic images, acoustic profiles and the histograms of samples obtained at 130°C and 160°C are shown in Fig. 7 and Fig. 8, respectively. As is evident the profiles and the histograms of these samples are quite different. Thus, the histogram of the sample obtained at 160°C is wider than that obtained at 120°C. The shift and the widening of histograms to the right indicate that the dimensions of the polystyrene inclusions have increased [1].

The following characteristics are usually of interest in a morphological analysis of similar structures:

– the number of grains in the field of view of the microscope and the coordinates of their mass centers; the ratio of the sum of grain areas to the sample area, i.e. percent ratio of components within the field of view;

– the areas, perimeters and the dimensions of the grains (maximal distance between points belonging to the grain), the criterion of the grain configuration;

– the homogeneity of the distribution of grain matter within the field of view of the microscope; calculation of the degree of the homogeneity.

And if the grains form agglomerated structures, in relation to the agglomerates, of interest are all the above-mentioned characteristics as well as data on the composition of each agglomerate: which grains are part of each agglomerate, the average number and dispersion of grains in the agglomerates.

We have worked out a series of software for calculating all these characteristics. We formed the criterion of homogeneity as the relation: $G = (\bar{S}^2/N)^{1/2}$; where, $\bar{S}^2$ – dispersion of the moving average (two-dimensional distribution of the average

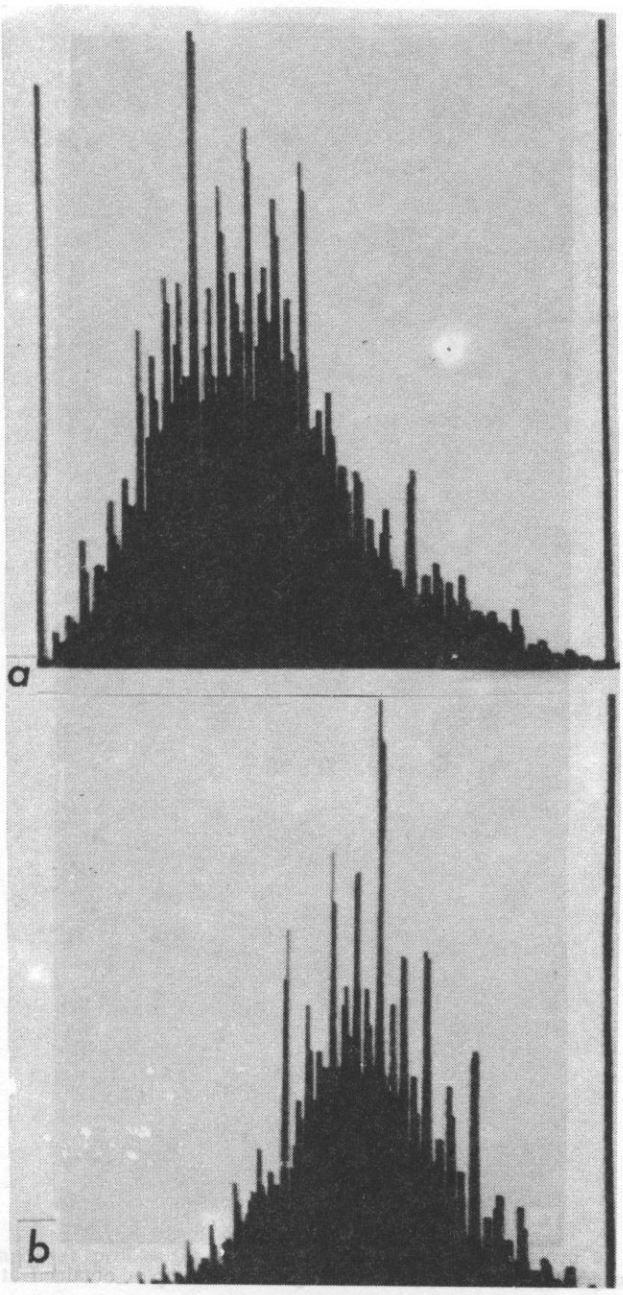

FIG. 6. Histograms of polymeric composites (a) and (b)

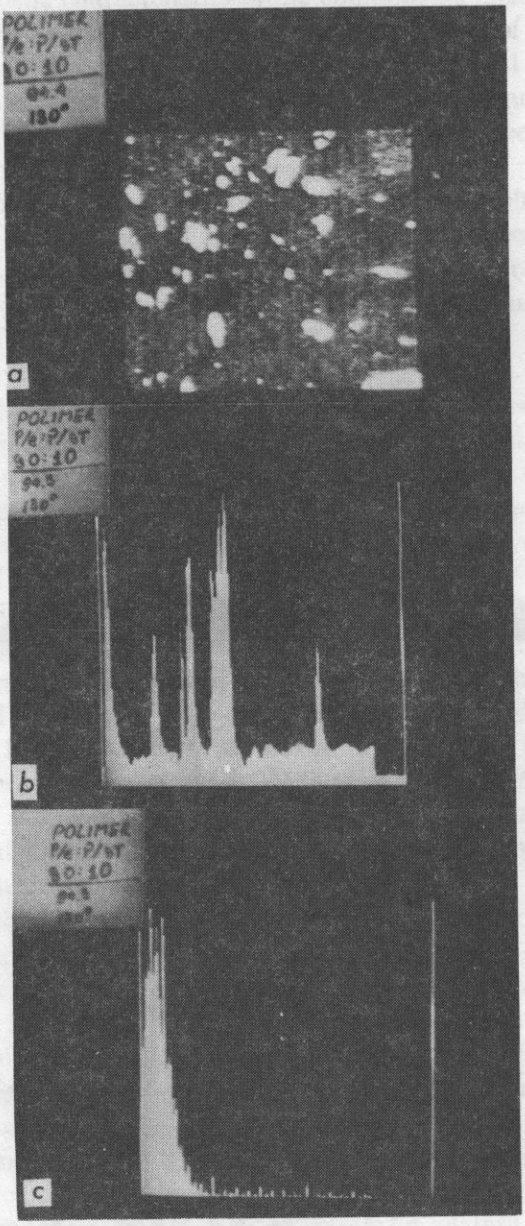

FIG. 7. Acoustic images (a), profiles (b) and histograms of samples obtained at 130°C, respectively

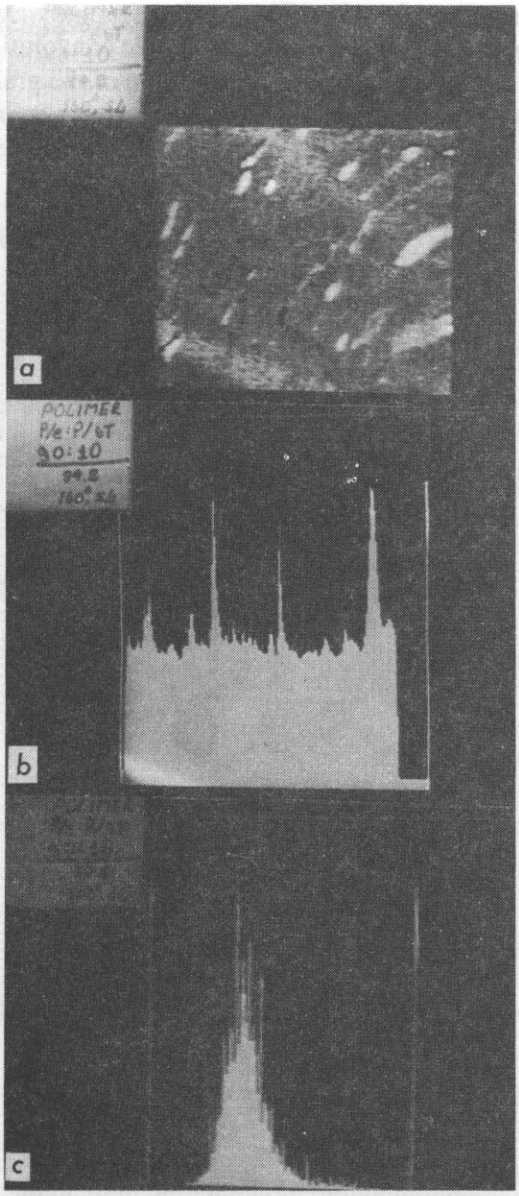

FIG. 8. Acoustic images (a), profiles (b) and histograms of samples obtained at 160°C, respectively

local value), N – normalized function. The moving average was determined from the equation $S(x, y) = q(x, y) * p(x, y)$; where $*$ – cyclic convolution, $p(x, y)$ – binary image, [$p(x, y) = 1$, if the point (x, y) belongs to one of the grains, in all other cases $p(x, y) = 0$;] $q(x, y)$ equal: $q(x, y) = 1$, if the point (x, y) belongs to the square of the area S_{sq} with the center at the zero of the coordinates system, in all other cases

FIG. 9. Result of threshold processing of acoustic image of polymeric composites

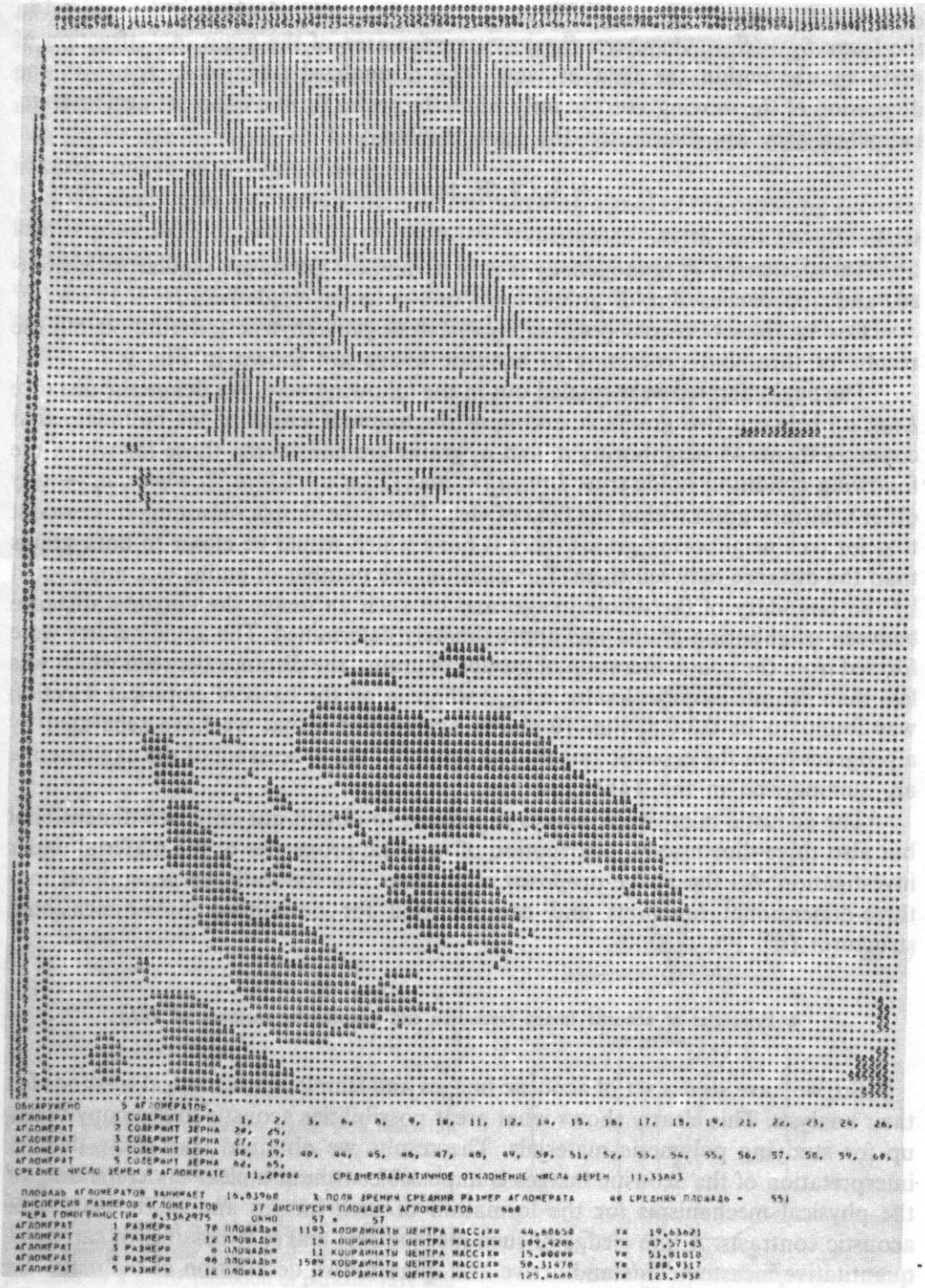

FIG. 10. Agglomerates that have been separated by a program from the acoustic image of polymeric composites

$q(x, y) = 0$. The average with respect to square, the area of which is determined in the form: $S_{sq} = \bar{S}_{\text{grain}}/\Delta$; where, $\bar{S}_{\text{grain}}$ – average area of the grain, Δ – fraction of grain matter within the field of view. The normalized function is equal to the dispersion of the moving average only when the grains form a coherent agglomerate, i.e., when they are distributed the least regularly:

$$N = [\bar{S}_n S_{sq}^2 \Delta(\Delta - 1)]^{1/2}$$

where $\bar{S}_n$ – area of the sample.

Thus, criterion of homogeneity is zero if identical grains are regularly distributed, and approaches zero if grains form one coherent agglomerate.

For samples of mixed polymers polystyrene-polyethylene (mixture 50:50) the results of threshold processing of acoustic image are shown in Fig. 9.

The agglomerates were singled out in the following way. We define the distance $L(a_i, a_j)$ between two grains, a_i and a_j as the minimal length of the boundary that connects them. As neighboring a_i and a_j grains are considered those for which the following condition holds true: $L(a_i, a_j) < \max[L(a_i, a_j), L(a_j a_k)]$, where, a_k – any other arbitrary grain within the field of view. From the simple reasoning it is evident that for true neighboring grains there is none which would be closer to both grains than the distance between them. For dilation, the number of grains was augmented by the boundary of the whole image, and on such an image the maximal distance between neighboring grains was approximately determined. The agglomerates were formed from the conglomeration of groups of grains, the distance between which was less than definite empirical value $\alpha L_{\max}$; where, α on the basis of empirical selection was found to be 0.3-0.5. Fig. 10 shows agglomerates that we have separated by a program from the acoustic image. The results of the processing of the agglomerate are summarized in the Table [3].

The acoustic microscope makes it possible to obtain not only two-dimensional but also three-dimensional distribution of acoustic properties of the material under investigation. All the above-proposed algorithms can naturally be generalized into three-dimensional functions and can be used for describing three-dimensional structures [4].

4. Principles of acoustic image formation and quantitative methods of SAM

So, we have seen a set of acoustic images and simple mathematical methods for their analysis. This clearly shows what great possibilities acoustic microscopy opens up for studying polymeric materials. The results we obtained also show that an interpretation of the acoustic images is impossible without a clear understanding of the physical mechanisms for the formation of such images and of the nature of acoustic contrasts. A knowledge of such mechanisms makes it possible to carry out quantitative measurements and arrive at a quantitative description of the materials under investigation. A comparison of the output signal of an acoustic microscope, its

amplitude and phase with the amplitude and the phase of the reference signal in liquid yields information on the velocity of sound, acoustic impedance, extinction and geometric characteristics of the sample, its thickness, curvature, and inclination angle of the surface.

So, let us now return to the subject of acoustic microscopy and consider how the acoustic image of a sample is formed.

We shall begin by considering how the outgoing signal of the receiving acoustic lens is produced in general. A piezoelectric transducer is used as a receiver. It is a linear receiver. For an electric signal to be generated in the transducer, the incident wavefront must be parallel to its surface; in other words, the acoustic rays after refraction on the lens surface must be normal with respect to the transducer's surface.

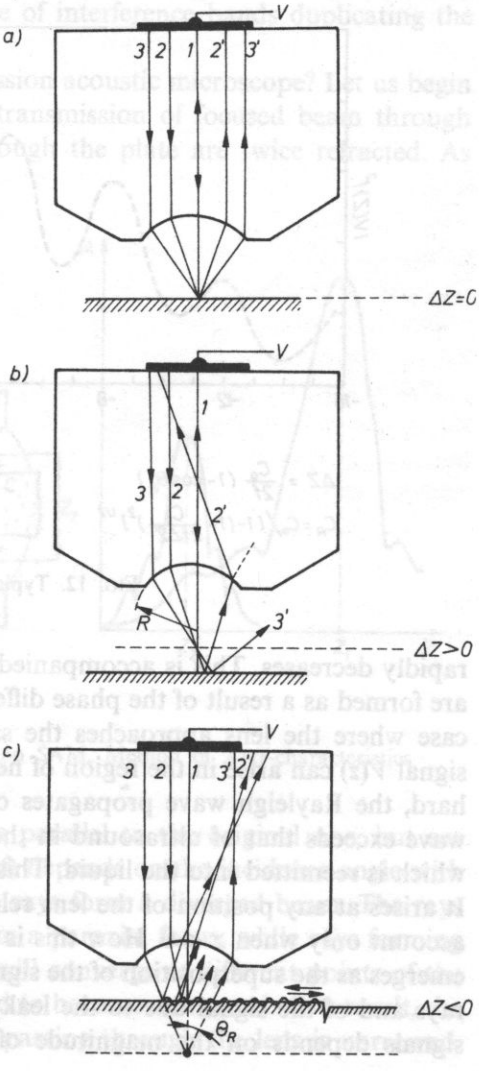

FIG. 11. Formation of output signal in a reflection SAM. z– the focal length of a lens. In case: a) $\Delta z = 0$ – output signal is formed by the integrity of all the refracted rays, b) $\Delta z > 0$ – only paraxial beams contribute to output signal, c) $\Delta z < 0$ – the output signal emerges as the superposition of the signal produced by a mirro–reflection of paraxial rays and of the signal due to the leaky surface Rayleigh wave

In addition, all incident rays reaching the transducer must be in the same phase. Otherwise, there will be interference of signals due to different rays, and the resulting signal will be weakened. First, we shall consider how a signal is formed in a reflecting microscope (Fig. 11). If the boundary of the sample lies in the focus, then the outgoing signal is determined by the integral refractive index for all incidence angles θ from $\theta = 0$ to $\theta = \theta_m$; where, θ_m – one half of the divergence angle (Fig. 11 a). If the lens is moved away from the sample (b), the cone of rays received by the transducer rapidly narrows down. Simultaneously the intensity of the signal entering the transducer decreases. Let us examine the curve describing the amplitude of the outgoing signal $V(z)$ as the function of the distance between the lens and the sample (Fig. 12). With an increase of z in the region $z > 0$ the intensity of the outgoing signal

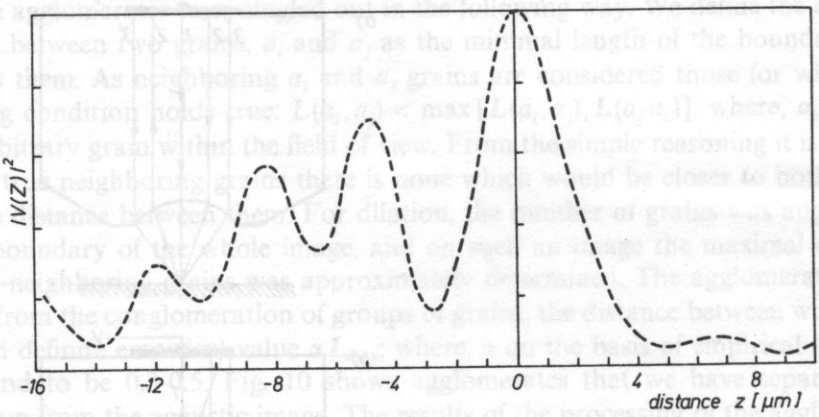

$$\Delta Z = \frac{C_0}{2f}(1-\cos\Theta_R)$$

$$C_R = C_0/[1-(1-\frac{C_0}{2f\Delta Z})^2]^{1/2}$$

FIG. 12. Typical $V(z)$-characteristic

rapidly decreases. This is accompanied by finely divided, shallow oscillations which are formed as a result of the phase difference of rays following different paths. In the case where the lens approaches the sample, a different dependence of the output signal $V(z)$ can arise in the region of negative values of z. If the sample is sufficiently hard, the Rayleigh wave propagates on its surface. If the velocity of the Rayleigh wave exceeds that of ultrasound in the immersion liquid, a surface wave is formed which is reemitted into the liquid. This is the so-called leaky surface Rayleigh wave. It arises at any position of the lens relative to the sample. However, it is taken into account only when $z < 0$. How this is done is shown in Fig. 11c. The output signal emerges as the superposition of the signal produced by a mirror reflection of paraxial rays and of the signal due to the leaky surface wave. The phase difference of these signals depends on the magnitude of the shift z: owing to their interference the

dependence $V(z)$ has a correct system of maxima and minima. The distance between the neighbouring maxima and minima is unambiguously related to the velocity of the Rayleigh wave on the surface of the sample [5]. The formation of the leaky surface Rayleigh wave is extremely important for the formation of acoustic images in the reflection mode. The formation of the leaky surface Rayleigh wave leads to the presence of interference bands in the vicinity of sharp heterogeneities and on distorted surfaces and so on. It is the cause of the inversion effect of acoustic contrast when there is a small shift of the lens. How interference bands are formed, for instance, near the defect in the sample surface is shown in Fig. 11c. Owing to the reflection from heterogeneities there arises not only a direct but also an inverse leaky surface Rayleigh wave which can also be received by the transducer. Since the phase of this wave depends on the position of the lens' axis relative to the heterogeneity, scanning of the lens leads to the appearance of interference bands duplicating the contour of the heterogeneity.

How is the image formed in the transmission acoustic microscope? Let us begin with the refraction effect and consider the transmission of focused beam through a thin plate (Fig. 13). The rays passing through the plate are twice refracted. As

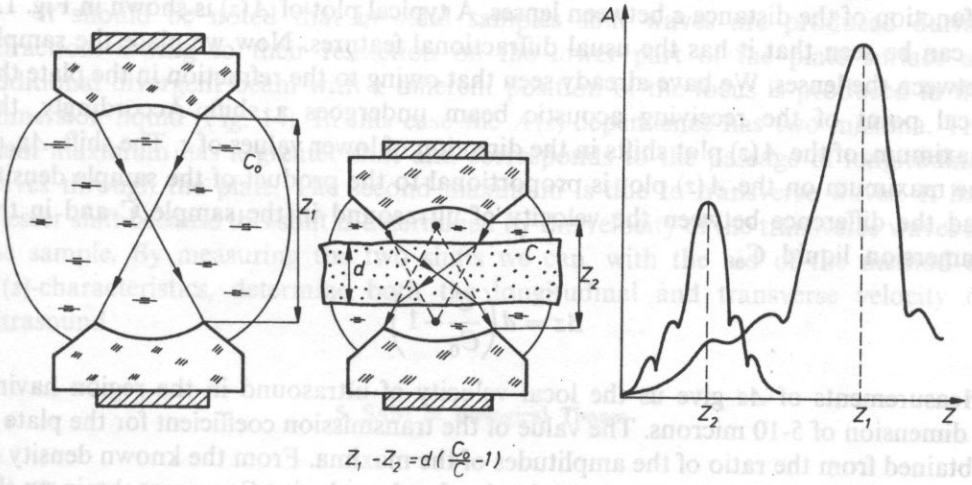

FIG. 13. Formation of output signal in transmission SAM. Method of $A(z)$-characteristics

a result, they leave the plate in the direction parallel to the original one, but are shifted relative to it. The magnitude of the shift depends on the incidence angle with the plate. After passing through the plate the rays form a diverged beam. The rays passing close to the lens axis converge to form a paraxial focus; while rays forming large incidence angles with the plate surface will converge at different points of the acoustic axis. This causes the focus to shift and to become defocused. As a result, the cone of rays received by the transducer after passing through the lens is narrowed,

and the output signal becomes less intense. Changes in the intensity of the signal due to the refraction effect will be determined by the ratio of the ultrasound velocity in the sample to that in the liquid. In an analogous way the rays cone registered by the receiving lens will become narrow owing to phase aberrations. These aberrations are explained by the fact that incident rays at different angles to the sample travel along different paths in the sample. Therefore, the rays have different phases and can mutually weaken the signals generated by them in the output piezoelectric transducer. The magnitude of phase aberrations is also determined by the difference of sound velocity in the liquid and in the sample. Therefore, the phase aberrations cause an additional contrast of acoustic images. There is yet another source of acoustic contrast, namely the reflection at both ends of the sample. This reflection depends on the magnitude of acoustic impedance at the observation point. For samples whose acoustic impedance differs slightly from that of water, such mechanism of acoustic contrast is of little significance. For such samples as polymers and biological tissues the formation of acoustic images is mainly due to the difference in local attenuation of sound.

In order to establish quantitatively the local mechanical properties of the sample we have developed a new special method of $A(z)$-characteristics [4]. Plot $A(z)$ describes the dependence of the output signal A of the receiving lens as a function of the distance z between lenses. A typical plot of $A(z)$ is shown in Fig. 13. It can be seen that it has the usual diffractional features. Now we place the sample between the lenses. We have already seen that owing to the refraction in the plate the focal point of the receiving acoustic beam undergoes a shift. Accordingly, the maximum, of the $A(z)$ plot shifts in the direction of lower values of z. The shift, Δz, of the maximum on the $A(z)$ plot is proportional to the product of the sample density and the difference between the velocity of ultrasound in the sample C and in the immersion liquid C_0.

$$\Delta z = d\left(\frac{C}{C_0} - 1\right).$$

Measurements of Δz give us the local velocity of ultrasound in the region having a dimension of 5-10 microns. The value of the transmission coefficient for the plate is obtained from the ratio of the amplitudes of the maxima. From the known density of the sample ϱ and by using the derived value for the velocity C, we can obtain on the basis of the known values of impedance and the transmission coefficient – the local coefficient of ultrasound attenuation. By using the method of $A(z)$–characteristics we measured the velocity of ultrasound in thin polymer films. For this we used films made of polyarylate and its block copolymer silar. The thickness of the films varied in the range 9–17 μm. For the samples of polyarylate the velocity of ultrasound was found to be 2,710 and for silar 1,020 km/s, respectively. A knowledge of these parameters makes it possible, in principle, to investigate the distribution of the local physico-mechanical properties of these materials within a wide range of concentrations.

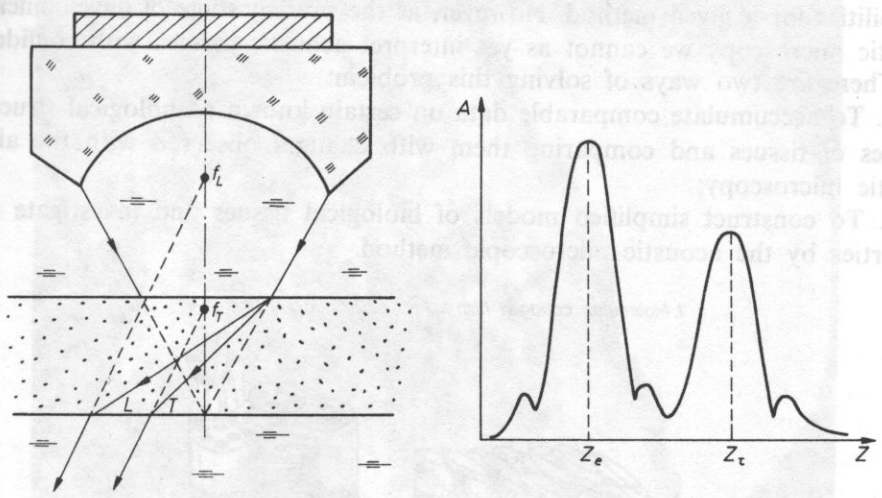

FIG. 14. Formation of two maxima of microscope output signal: for longitudinal waves (L) and shear waves (T)

It should be noted that in solid samples shift waves are produced during refraction. Owing to their refraction on the lower part of the plate surface an additional divergent beam with a different position of the focus is produced in the immersion liquid (Fig. 14). In this case the $A(z)$-dependence has two maxima. The main maximum has a greater shift and corresponds to the passage of longitudinal waves through the plate. The second maximum is due to transverse waves. It has a lesser shift because this shift is determined by the velocity of the transverse waves in the sample. By measuring the two shifts we can, with the aid of the method of $A(z)$-characteristics, determine both the longitudinal and transverse velocity of ultrasound.

5. SAM of Biological Tissues

The development of the quantitative methods of scanning acoustic microscopy opens up great possibilities for research in one more area: the study of the viscoelastic properties of biological materials on a histological and cytological level. For already more than 10 years scanning acoustic microscopy has been used in biological research.

The experience gained to date in interpretation acoustic images of collagen tissues shows that the contrast provided by acoustic microscopy depends on the size of the collagen fibers, their density and water-content, and the degree of order and orientation of the fibers relative to the observation axis (Fig. 15). The fact that there is such a large number of parameters affecting the contrast opens up wide diagnostic

possibilities for a given method. However, at the present stage of development of acoustic microscopy we cannot as yet interpret acoustic images with confidence.

There are two ways of solving this problem:

1. To acccumulate comparable data on certain known pathological structural changes of tissues and comparing them with changes observed with the aid of acoustic microscopy;

2. To construct simplified models of biological tissues and investigate their properties by the acoustic microscopic method.

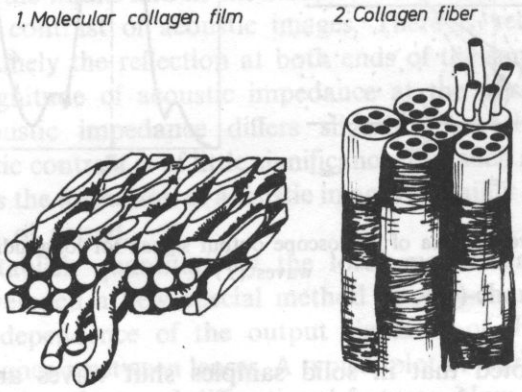

Materials
Molecular collagen films were formed by drying acetic acid solution of molecular pig skin collagen at 4°C during 48 hours. Collagen fibers from rat tail tendon were under study. 10 μ collagen fibers were prepared using kryotome Leitz 1321.

FIG. 15. Structure of various collagen fibers

The first approach requires extensive acoustic microscopic studies of pathological tissues.

In our work we devoted most of our attention to a study of the viscoelastic properties of models of collagen-rich tissues. First we studied the acoustic images of normal tissues. (Fig. 16). This figure shows the acoustic and optical images of a lateral slice of human skin. The acoustic image was obtained in our laboratory with the aid of transmission acoustic microscope [1] operating on a frequency of 450 HMz and having a resolution of 3μm. The sample, 7μm thick, was in a non-fixed position and was not treated with a dye. The picture gives a good view of three layers. The first is a dark band in the surface of skin is the corneous layer. It consists of a densely packed keratin protein. Then follows an acoustically transparent layer of epithelian cells. And finally there is a structurally heterogeneous derma, which is a dense network of collageneous and elastinic fibers submerged into an intercellular liquid.

There is a general similarity of acoustic and optical picture. Outlines of the objects and boundaries of shape inhomogeneities coincide on both images. One may suppose that the contrast of acoustic images on this picture is determined by the

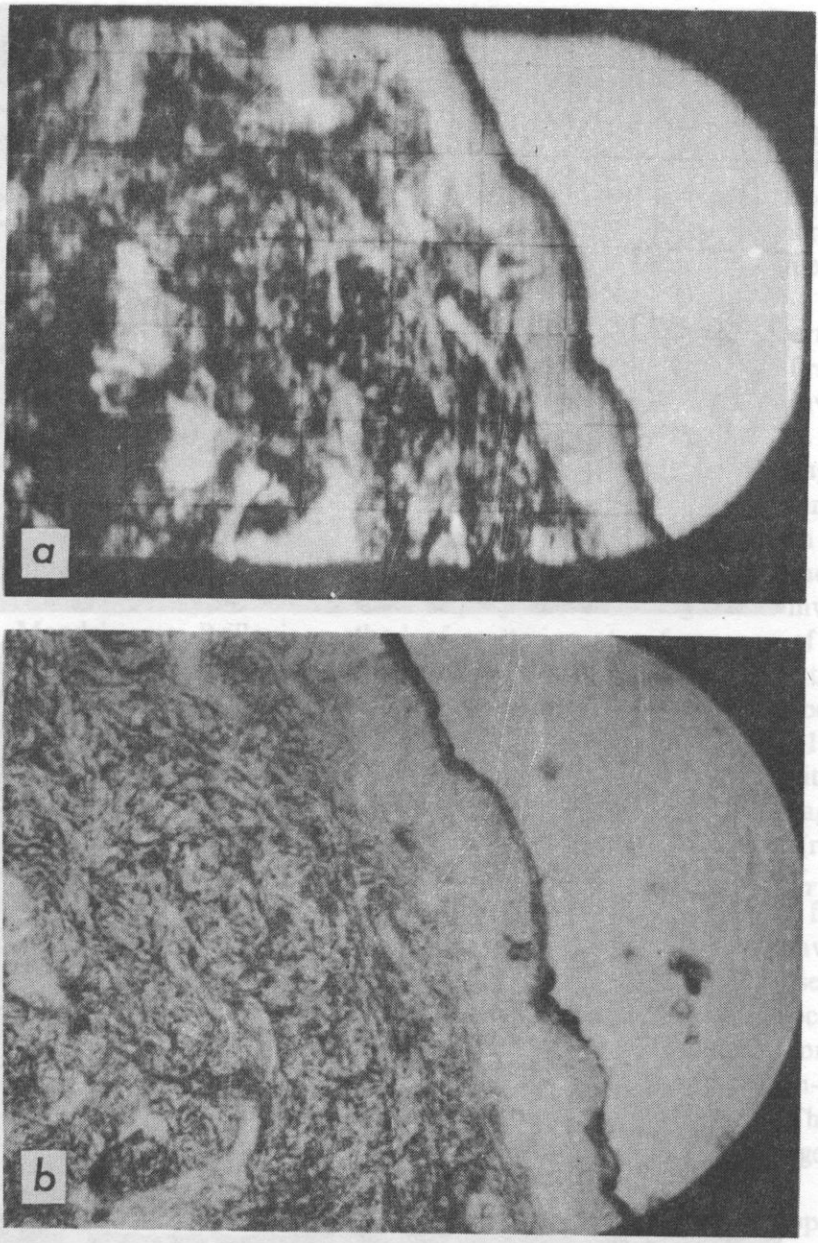

FIG. 16. Acoustic (a) and optical (b) images of a slice of human skin

magnitude of the local coefficient of attenuation of ultrasound in soft tissues correlates with the concentration of fibrilar protein in them. Therefore, a system of dark and light regions in acoustic image should reflect the distribution of collagen (or keratin) in the sample. For a quantitative evaluation we can use the acoustic profile (Fig. 17). In this Figure we can see a liver slice image with bubble air and two vessels

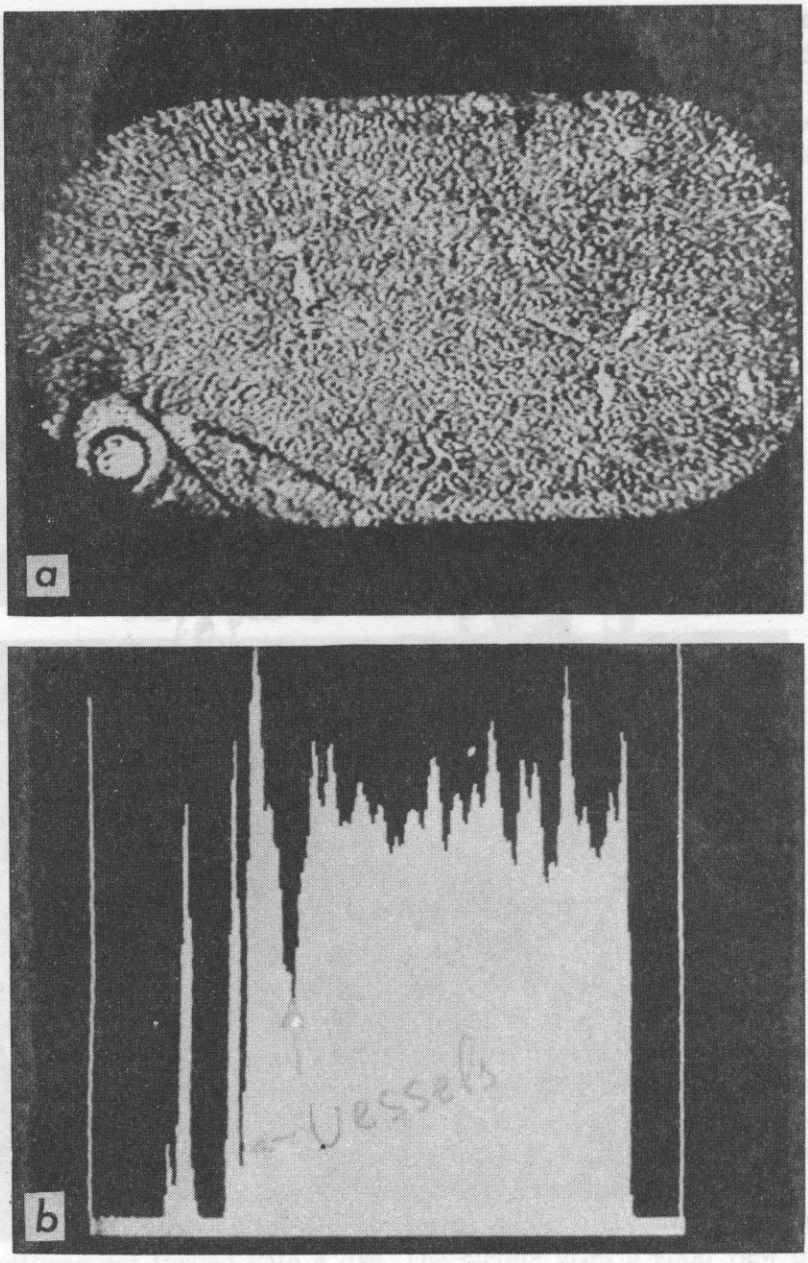

FIG. 17. Acoustic image and profile of liver slice (with the air bubble and two vessels)

and profile, which can give us a precise information. Using this profile as in polymers case we can determine the local concentration of collagen and arrive at a quantitative description of collagen inside the tissue. And herein lies our main difficulty: we can provide a quantitative description of the distribution but we have yet to find a biologist or medical specialist who would be interested in such a description.

Figure 18 shows acoustic and optical images of a longitudinal and a transverse slice of a human sclera. The poor definition of the optical images is due to the fact that the sample was in a non-fixed state and undyed. In both the acoustic and optical images one can see packed bundles of collagen fibers. On the optical image one can see only the outline of the boundaries of the fibers; while on the acoustic image one can see different gradations of grey coloring, which makes it possible to decipher the density of the fibers and the local concentration of collagen. Numerically the concentration of collagen can be estimated by using acoustic profiles as was mentioned above.

Since the acoustic properties of tissues are determined by the properties of the components of the tissues and their mutual orientation, we are interested first of all in the mechanical properties of the components, collagen in particular. We investigated mechanical properties of collagen-fibers with our acoustic microscope. Different authors (Fig. 19) have measured velocity of ultrasound along the entire length of the fiber ($V_s = 2.1$ km/s) and across it ($V_s = 1.73$ km/s) by means of a scanning laser acoustic microscope operating at a frequency of 100 MHz (wavelength in water $\sim 15\mu$m). These results indicate a strong anisotropy of the elastic modules of collagen. The anisotropy of the viscoelastic properties of collagen was investigated by the Mandelstamm-Brillouin method of scattering at a frequency of 10 GHz (wavelength in water $\sim 0.15\mu$m). Measurements of the longitudinal and transverse waves yielded five values of elastic constants for partially dried collagen fiber, on the assumption that collagen is a transversely masotrophic medium (Fig. 19).

By using the values of these constants we calculated the velocity of the longitudinal and transverse waves propagating at different angles in collagen fiber. Fig. 20 shows the slowness of surfaces of acoustic waves in collagen (reciprocal velocities $1/V_L$, $1/V_T$; where V_L – phase velocity of the longitudinal wave, V_T – phase velocity of the shear wave. Here, the z axis corresponds to the axis of the fiber. The results show a strong anisotropy in the velocity of the longitudinal wave (phase velocity of the longitudinal wave along the fiber $V_{L\parallel} = 3.64$ km/s, phase velocity across the fiber $V_{L\perp} = 2.94$ km/s) and a rather weak anisotropy in the velocity of the shear wave ($V_{T\parallel} = V_{T\perp} = 1.563$ km/s, $V_T = 1.639$ km/s at 49° angle). For natural collagen fiber the transverse mode in the spectrum of Mandelstamm-Brillouin scattering was absent; i.e., there was no propagation of the shear waves. This means that there is a strong dependence of the viscoelastic properties of collagen on its saturation with water.

All the above-mentioned factors – the dependence of the elastic properties on the direction and packing density of fibers and their size, and water concentration – contribute to a certain extent to the contrast of the acoustic images of tissues.

To elucidate the particular effect of each of these parameters we carried out our studies on modeled systems.

The simplest model of a collagen tissue slice is a homogeneous layer. We examined the gelatin-collagen layers in the dehydrated state. The layers were formed from molecular solutions of collagen in which the molecules were positioned with their long axis being in the plane of the layer.

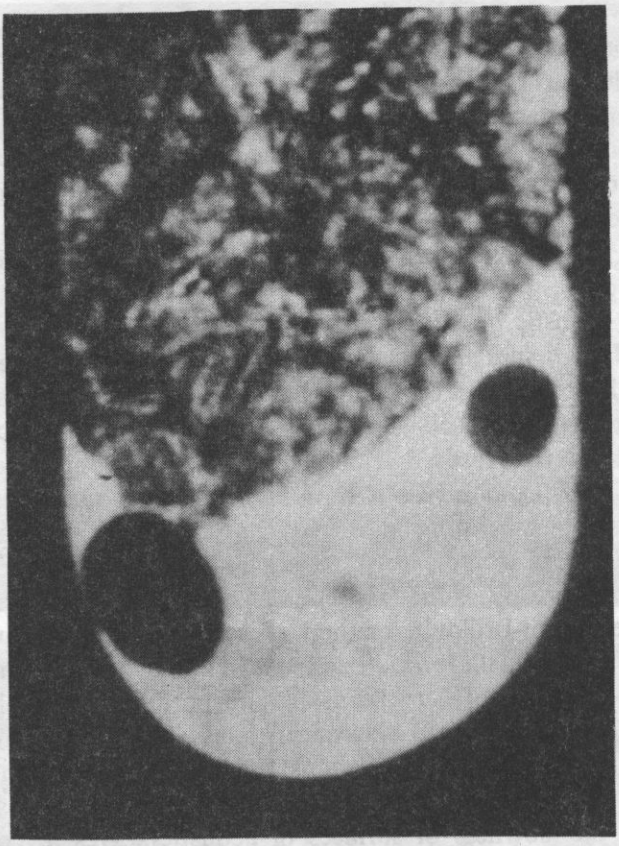

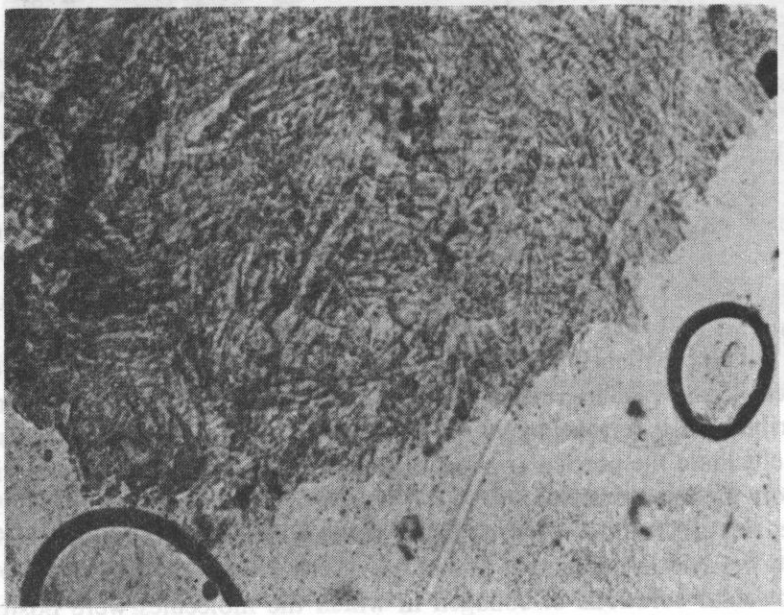

a

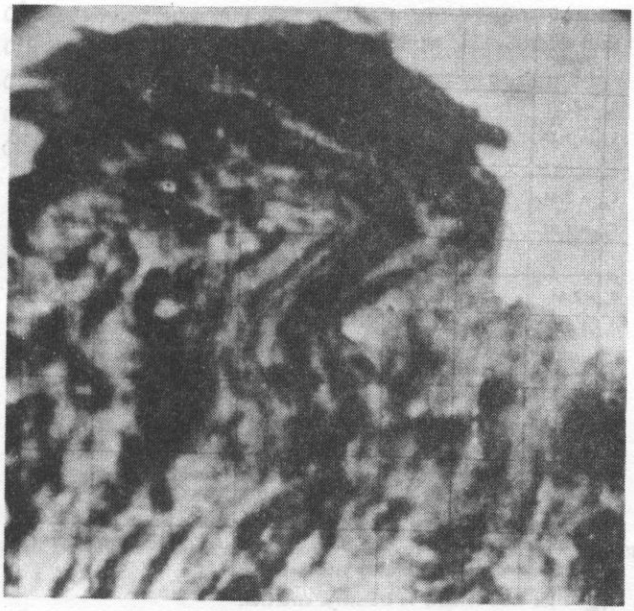

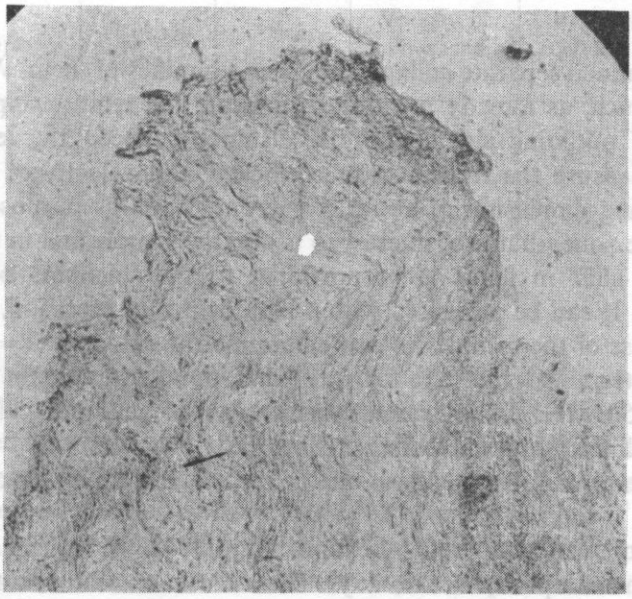

b

FIG. 18. Acoustic and optical images of a longitudinal (a) and a transverse (b) slice of a human sclera

SOUND VELOSITY, KM/SEC	THE METHOD	AUTHORS	OBJECT
C_{ax}= 2.11 C_{rad}= 1.73	SLAM 100 MHz	S.LEES, J.HEELEY, J.AHERN	FIBERS OF RAT'S TAIL TENDON
C_{ax} = 2.64 C_{rad}= 1.89	BRILLOUIN LIGHT SCATTERING 10 GHz	HARLEY, D.JAMES, A.MILLER	FIBERS OF RAT'S TAIL TENDON
C_{ax}= 2.64 C_{rad}= 1.89	BRILLOUIN LIGHT SCATTERING 10 GHz	CUSAK S. MILLER A.	FIBERS OF RAT'S TAIL TENDON
C_{ax} = 1.82 C_{rad}= 1.69	IMPULS ECHO technique 10 MHz	S.LEES, J.HEELEY P.CLEARY	FIBERS OF BOVINE TI- BIA MATRIX
C = 1.73 without specifing direction of propagation	SLAM 100 MHz	S.GOSS W.D.O'BRIEN	FIBERS OF MOUSE TAIL TENDON

C_{ax} is the sound velocity along the fiber axis.

C_{rad} is the sound velocity in transverse direction.

FIG. 19

Next we examined separate collagen fibers and bundles of them. With the aid of the $A(z)$ plots which, as already mentioned, indicate the relationship between the amplitude of the outgoing signal and the distance between the lenses, we can simultaneously measure the transmission coefficient and velocity of sound within a local zone having dimension of about 5 microns. For this purpose we plot the $A(z)$-graph for the zone (that is of interest to us) on the sample and in the absence of the sample. The shift in focus is proportional to the thickness of the sample: $\Delta z = d(C/C_0 - 1)$. It can be measured with a high degree of precision, and, since we know the thickness of the sample we can determine the velocity: $C = C_0(\Delta z/d + 1)$.

We have determined the velocity and ultrasound attenuation coefficient at a frequency of 450 MHz in a 2-micron-thick layer of gelatin, a 10-micron-thick collagen film and in 10-micron collagen fiber [4].

A gelatin film of uniform thickness can be separated from a photo film in water at $t = 90°C$.

Collagen films were prepared by evaporating at 4°C a molecular solution of pig's skin collagen for a period of two days. The molecular solution was obtained by extracting collagen from pieces of pig's skin with a 0.1 M solution of glacial acetic acid followed by precipitation of protein with cooled ethanol.

Collagenous fibers were separated from the longitudinal slices of the tendon from a rat's tail. The slices were obtained on a refrigerated Leitz microtome, the temperature of the table and the knife $T = -20°C$.

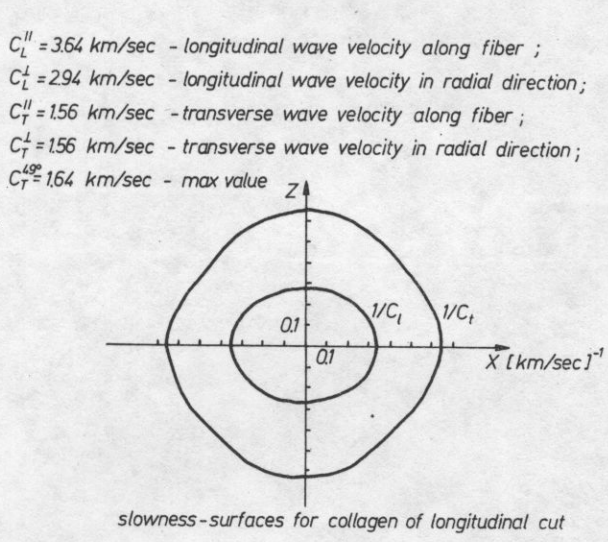

FIG. 20. Grafics of slowness-surfaces of acoustic waves in collagen

Table 1

Sample	Thickness [μm]	Density [g/cm^3]	Velocity of ultrasound [km/s]	Attenuation coef. (10^{-17}) [s^2/cm]
Gelatin	2	1.2	2.9±0.3	420±40
Collagen film	10	1.3	2.4±0.3	445±45
Collagen fiber	10	1.35	2.8±0.3	660±60

In Tab. 1 there are summarized the values for the ultrasound velocity and attenuation coefficients for these samples measured at 450 MHz.

The proposed approach can be regarded only as an initial stage in obtaining the quantitative characteristics of the local viscoelastic properties of tissues. However, even now this method enables us to estimate the effect of a number of parameters, such as the pH, temperature, etc, on the biochemical properties of tissues.

In this report I have described the results of first steps of acoustic microscopic research performed in our Center in only two fields: the physics of polymeric mixtures and biophysics. The various experimental results obtained with the aid of the transmission microscope, and the wide possibility of obtaining quantitative data with this microscope, in our opinion, convincingly demonstrate the rich scientific potentialities inherent in the principle of raster acoustic microscopy.

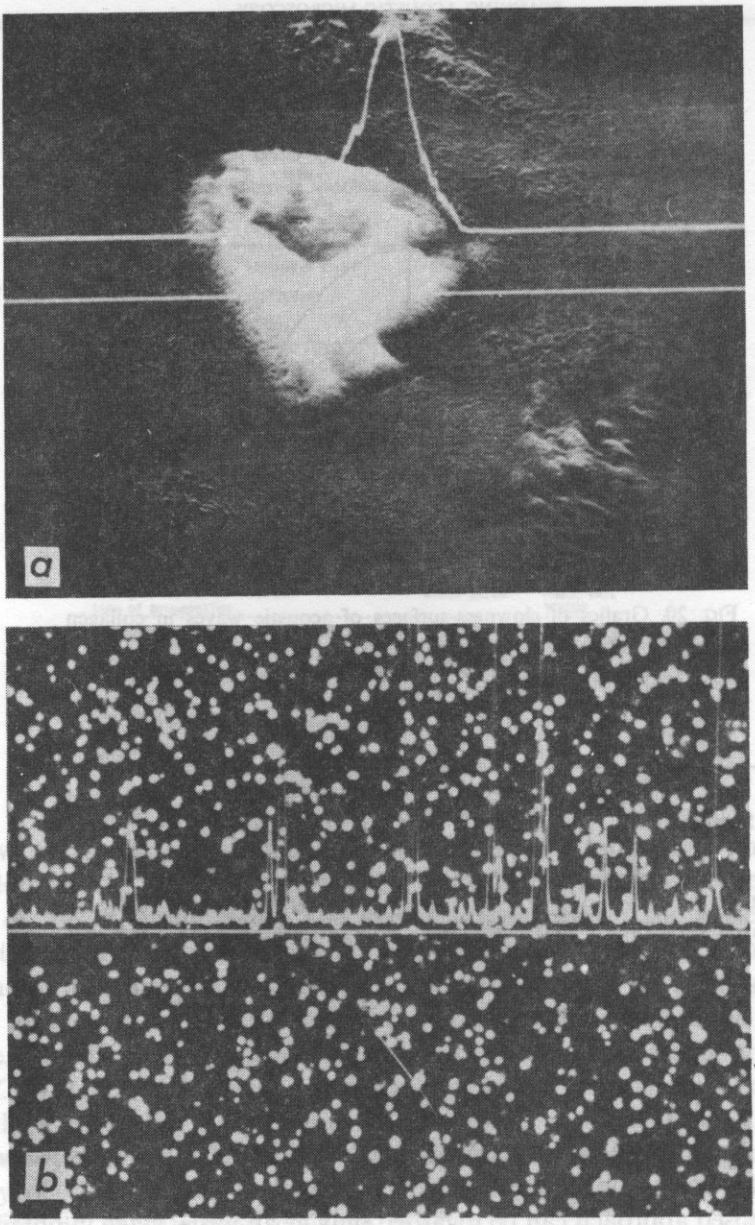

FIG. 21. Acoustic images of different materials. a) laminated structure ($SiO_2-Si-SiO_2$-substrate-Si) $f = 0.4$ GHz. Degree of penetration $\Delta z = -10$ μm. The microscope is focused on the boundary between the substrate and the layer to a depth of 10 μm from the sample surface reflecting optical rays. The acoustic image shows a defect at the interface. The same is confirmed by the one-dimensional profile of the refracted signal amplitude along the scanning line, marked on the photo; b) a photo film, representing the celluloid base, coated by gelatin matrix with silver crystals of $2 \div 3$ μm. Frequency $f = 1.3$ GHz. The image was obtained in the layer close to the surface $\Delta z = -0.5$ μm. One of the parameters determining the quality of photomaterials is the homogeneity degree of silver grains distribution in the matrix, their relative orientation, the absence of agglomerates etc. Optical methods do not allow to carry out such an analysis due to the specific nature of the object. Such a control can be timely realized by SAM methods. Since the acoustic properties of silver crystals differ greatly from those of the matrix and the immersion

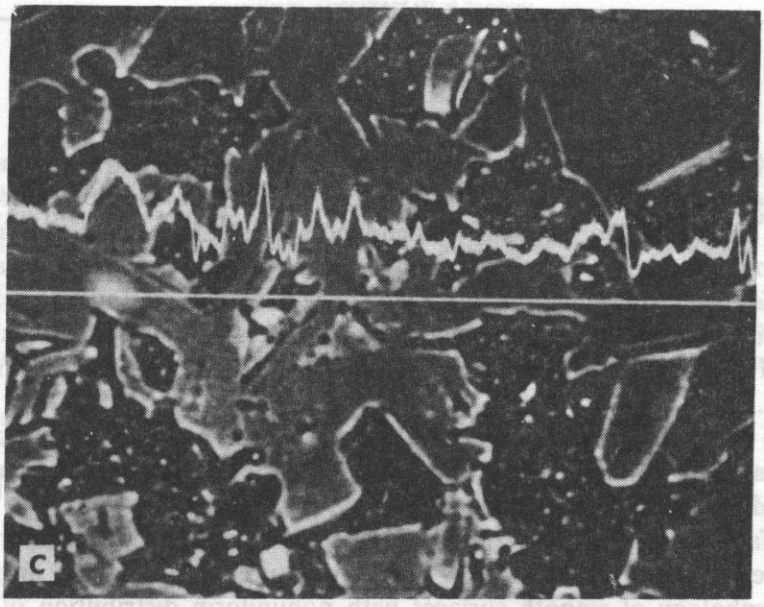

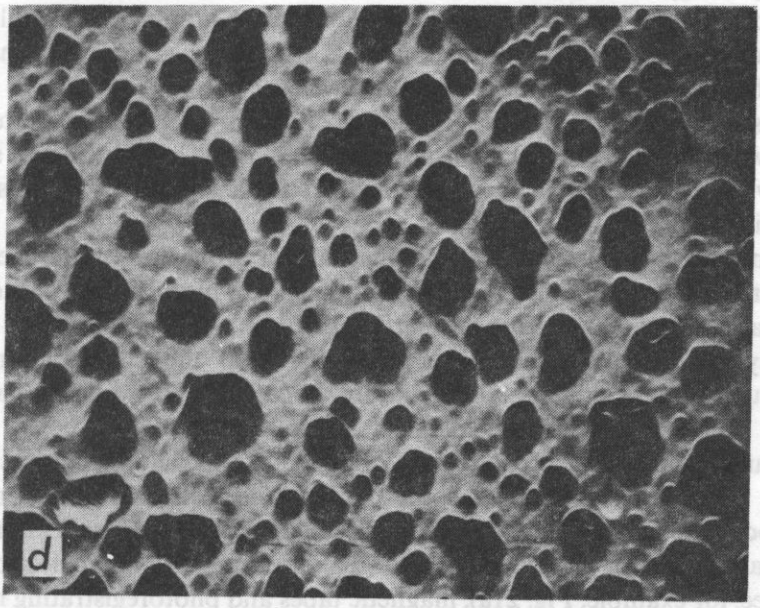

media, the image obtained is highly contrasting and its information content is very high. The profile of the refracted signal amplitude along the scanning line, marked on the photo, was applied to the image; c) high-temperature superconducting ceramics. $f = 1.3$ GHz, focal length $\Delta z = -2\mu$m. At the depth of 2 μm of optically non-transparent material one can clearly see the structure of ceramics with sharp boundaries of pores between crystals and the inner structure of pores. The profile of the refracted signal amplitude along the scanning line, marked on the photo, was applied to the image; d) polymer composite (polyacrylate-silar-rubber). $f = 1.3$ GHz. Focal length $\Delta z = 5$ μm. The photo clearly displays the distribution of the two types of fillers (large-sized and finely divided) in the polymer matrix at the depth of 5 μm (Acoustic images were obtained by the specialists from the Center of Acoustic Microscopy, the USSR Academy of Sciences, O. V. Kolosov, L. F. Matsiev and T. A. Senyushkina)

6. Practical Applications of Acoustic Microscopy

The method of acoustic microscopy turns out to be very sensitive to the presence in the object of any kind of inhomogeneities as well as to the disturbance of uniformity, since due to acoustic impendances mismatch there appear strong reflections on boundaries. At the present time the acoustic microscopy allows to reveal the following defects: adhesion disturbance, exfoliations microcracks pores, foreign inclusions, deviations from the given thickness of the layer in multilayered system and coatings, technological deviations of sizes, orientation and grain distribution.

So, the following trends in the development of the methods of refraction and transmission acoustic microscopy for the investigation of surface and subsurface structures, different materials seem to us very perspective:

– surface topography (determination of steps height, the width of cracks and the character of stress fields around them, curvature radius, wedge angles etc.);

– morphology of smooth surfaces with nonuniform distribution of acoustic properties (characterization of separate components of granular and multilayered structures, acoustic images of internal planes, structures, grains, the analysis of thin-filmed heterogeneous objects);

– measurements of local values of the velocity of propagation and attenuation of Rayleigh waves in materials by acoustic microscopy using cylindrical and spherical lenses; study of distribution of local anisotropic elastic properties of crystals and other materials;

– quantitative measurements of nonmechanical properties by the methods of acoustic microscopy, among them local measurements of piezoelectric, photoelectric, high-temperature superconducting properties of films;

– study of dynamic phenomena connected with the change in materials properties due to physical factors (temperature, UV-, IR-, SHF-radiation) as well as mechanical, chemical and pharmacological factors.

The results, which have been recently obtained in this field, allow to state that the acoustic microscopy methods become the working instrument of scientist and engineer. Today we can speak about the first concrete practical applications of the method: quality control of semiconductor engineering and microelectronics instruments (see, for example, Fig. 21a), magnetic tapes and photoregistrating materials (Fig. 21b), technological and physicomechanical control of alloys, ceramics (Fig. 21c), polymeric composite materials with optically close or nontransparent components (Fig. 21d), poly- or monocrystalline films, adhesive joints, seams, reinforcing and protective coatings, antireflecting and paint and varnish layers, biomedical objects and some others.

References

[1] *Proceedings of the first joint Soviet-West Germany Int. symp. on microscope photometry and acoustic microscopy in science*, [Ed.] R. G. Mayev, M. Hoppe, Moscow 1985.

[2] N. S. Enikolopian, O. V. Kolosov, E. Yu. Lagutenkova, R. Gr. Mayev, D. D. Novikov, *Investigations of heterogeneity of polymeric composite materials by methods of acoustic microscopy*, Soviet physics, Doklady **292**, 6, 1418–1422 (1987).

[3] L. A. Piruzyan, O. V. Kolosov, R. Gr. Mayer, V. M. Levin, T. A. Senyushkina, *Acoustic microscopy of organic and biological materials*, Soviet Physics. Doklady, **280**, 4–6, 1115–1117 (1985).

[4] *Proc. of the 5-th Soviet-West Germany symp. on new methods for microscopy in biology and medicine*, Moscow 1987, 141–151.

[5] A. Briggs, *An introduction to scanning acoustic microscopy*, Microscopy handbooks 12, Alden Press Oxford 1985.

[6] O. V. Kolosov, V. M. Levin, R. Gr. Mayev, T. A. Senyushkina, *The use of acoustic microscopy for biological tissue characterization*, Ultrasound in Medicine and Biology, **13**, 8, 477–483 (1987).

Received on January 25, 1988